



Two mutations in the ORF1 of genotype 1 hepatitis E virus enhance virus replication and may associate with fulminant hepatic failure

Bo Wang^{a,b} , Debin Tian^{a,b} , Harini Sooryanarain^{a,b}, Hassan M. Mahsoub^{a,b} , C. Lynn Heffron^{a,b}, Anna M. Hassebroek^{a,b} , and Xiang-Jin Meng^{a,b,1}

Contributed by Xiang-Jin Meng; received April 30, 2022; accepted July 16, 2022; reviewed by Sébastien Lhomme and Daniel Todt

Hepatitis E virus (HEV) infection in pregnant women has a high incidence of developing fulminant hepatic failure (FHF) with significant mortality. Multiple amino acid changes in genotype 1 HEV (HEV-1) are reportedly linked to FHF clinical cases, but experimental confirmation of the roles of these changes in FHF is lacking. By utilizing the HEV-1 indicator replicon and infectious clone, we generated 11 HEV-1 single mutants, each with an individual mutation, and investigated the effect of these mutations on HEV replication and infection in human liver cells. We demonstrated that most of the mutations actually impaired HEV-1 replication efficiency compared with the wild type (WT), likely due to altered physicochemical properties and structural conformations. However, two mutations, A317T and V1120I, significantly increased HEV-1 replication. Notably, these two mutations simultaneously occurred in 100% of 21 HEV-1 variants from patients with FHF in Bangladesh. We further created an HEV-1 A317T/V1120I double mutant and found that it greatly enhanced HEV replication, which may explain the rapid viral replication and severe disease. Furthermore, we tested the effect of these FHF-associated mutations on genotype 3 HEV (HEV-3) replication and found that all the mutants had a reduced level of replication ability and infectivity, which is not unexpected due to distinct infection patterns between HEV-1 and HEV-3. Additionally, we demonstrated that these FHF-associated mutations do not appear to alter their sensitivity to ribavirin (RBV), suggesting that ribavirin remains a viable option for antiviral therapy for patients with FHF. The results have important implications for understanding the mechanism of HEV-1-associated FHF.

hepatitis E Virus (HEV) | genotype 1 HEV (HEV-1) | fulminant hepatic failure (FHF) | FHF-associated HEV-1 mutations | genotype 3 HEV (HEV-3)

Hepatitis E virus (HEV), the causative agent of hepatitis E, is one of the most common causes of acute viral hepatitis worldwide (1). Although the majority of HEV infections are asymptomatic, HEV can cause severe liver diseases under specific circumstances. For instance, HEV infection in pregnant women shows rapid virus replication and has a high incidence of developing fulminant hepatic failure (FHF)/acute liver failure (ALF) with a mortality rate of up to 30% (2, 3). Additionally, the majority of HEV infections in immunosuppressed individuals, such as solid organ transplant recipients, can progress into chronicity, leading to liver fibrosis, cirrhosis, and death (4). Ribavirin (RBV) is commonly administered as an off-label treatment for chronic hepatitis E (CHE), but significant side effects often limit its use (5, 6). In addition to FHF and CHE, HEV is also associated with a wide range of extrahepatic manifestations (7). HEV-associated FHF, CHE, and neurological sequelae all require effective antiviral therapy, but unfortunately, an HEV-specific direct-acting antiviral is still lacking.

HEV is the prototype of the species *Paslabepavirus balayani* in the family Hepeviridae (8), whose members infect a broad range of mammals, including humans, domestic pigs, wild boars, deer, rabbits, and camels (9, 10). Eight distinct HEV genotypes within the species *P. balayani* thus far have been assigned; among them, genotypes 1 through 4 (HEV-1 to HEV-4) are major human-infecting variants with different geographical distribution, infection patterns, and clinical course (1, 10, 11). HEV-1 and HEV-2 exclusively infect humans and are transmitted through the fecal–oral route via drinking contaminated water in developing countries. In contrast, HEV-3 and HEV-4 are zoonotic and transmitted mainly through the food-borne route via consuming undercooked animal meats in industrialized nations. Of note, HEV-1 is responsible for large outbreaks and causes FHF, especially in pregnant women in endemic areas, whereas the vast majority of CHE is associated with zoonotic HEV-3 infection (9, 11). The genotype-specific evolution of HEV with different viral fitness and host range is not fully understood (12).

Significance

Infection with HEV-1 causes FHF, especially in pregnant women. Eleven amino acid changes in HEV ORF1 have been detected in variants from FHF patients. We comprehensively analyzed all FHF-associated mutations in silico and in vitro and investigated the effect of these mutations on replication efficiency and infectivity of HEV-1 and HEV-3. We identified two mutations, A317T and V1120I, that greatly enhanced HEV-1 replication individually or in combination, presumably contributing to increased viremia and poor clinical outcome. In contrast, all mutations reduced HEV-3 replication ability and infectivity, suggesting that genotype heterogeneity plays a role in disease severity. None of the mutations altered the sensitivity to ribavirin treatment. The finding will aid in our understanding of the mechanism of HEV-1-associated FHF.

Author contributions: B.W. and X.-J.M. designed research; B.W., D.T., H.S., H.M.M., C.L.H., and A.M.H. performed research; B.W. analyzed data; B.W. wrote the paper; and X.-J.M. revised the manuscript.

Reviewers: S.L., Université Toulouse III-Paul Sabatier; and D.T., Ruhr Universität Bochum.

The authors declare no competing interest.

Copyright © 2022 the Author(s). Published by PNAS. This article is distributed under Creative Commons Attribution-NonCommercial-NoDerivatives License 4.0 (CC BY-NC-ND).

¹To whom correspondence may be addressed. Email: xjmeng@vt.edu.

This article contains supporting information online at <http://www.pnas.org/lookup/suppl/doi:10.1073/pnas.2207503119/-/DCSupplemental>.

Published August 15, 2022.

HEV is a quasi-enveloped virus with a positive-sense, single-stranded RNA genome of ~7,200 bases, which typically contains three partially overlapping open reading frames (ORFs): ORF1 encodes a nonstructural polyprotein with several confirmed or potentially functional domains, including methyltransferase (Met), Y domain, papain-like cysteine protease (PCP), hypervariable region (HVR), X domain, helicase (Hel), and RNA-dependent RNA polymerase (RdRp); ORF2 encodes the structural capsid protein; and ORF3 partially overlaps with ORF2 and encodes a multifunctional protein involved in virion morphogenesis and pathogenesis (13). A novel, small ORF4 within ORF1, induced by endoplasmic reticulum (ER) stress, has been identified in most strains of HEV-1 but not in other HEV genotypes (14).

Thanks to the successful establishment of reverse genetic systems and advancement of cell culture models in HEV research (15, 16), several HEV-3 RdRp amino acid mutations have been studied *in vitro* for anti-RBV resistance and are associated with altered viral replication, virulence, and antiviral sensitivity (17–22). However, currently, our knowledge regarding the functional role of HEV-1 mutations responsible for FHF, especially in infected pregnant women, is very limited. A case study has reported the existence of six unique amino acid changes, F179S, A317T, T735I, L1110F, V1120I, and F1439Y, in HEV genomes derived from six FHF patients in India (23). Another case study also from India has reported the presence of two other ORF1 mutations, C1483W and N1530T, in all (25/25) FHF patients but none (0/30) in acute hepatitis patients. Notably, patients with these two mutations exhibited significantly higher viral loads in clinical samples and more severe diseases (24). The same group later reported that three other mutations, V27A, D29N, and H105R, occurred in 16/16 FHF patients but in 0/16 acute hepatitis patients, and that V27A and D29N were associated with increased viremia in patients, while H105R was associated with decreased viremia (25). Altogether, a total of 11 HEV-1 mutations have been reportedly linked to patients with FHF in clinical case reports. However, the roles of these FHF-associated mutations in HEV replication or infection have not been experimentally verified.

In this study, we first conducted a comprehensive *in silico* analysis and identified the precise positions and epidemiological prevalence of the 11 FHF-associated mutations in different HEV genotypes. Subsequently, by utilizing indicator replicons and infectious clones of both HEV-1 and HEV-3, we systematically determined and compared the effect of these FHF-associated mutations on HEV replication and infectivity. Our data provide the experimental evidence that two FHF-associated HEV-1 mutations enhance HEV replication efficiency, which may correlate with severe liver diseases such as FHF in HEV-1-infected patients.

Results

Identification and Prevalence of FHF-Associated Amino Acid Mutations among Different HEV Genotypes. In total, 11 FHF-associated amino acid mutations were reported in clinical cases, including V27A, D29N, H105R, F179S, A317T, T735I, L1110F, V1120I, F1439Y, C1483W, and N1530T (23–25). To investigate the effect of these mutations on HEV replication *in vitro*, we comprehensively analyzed the available 953 complete HEV genomes in the GenBank database and precisely identified the 11 FHF-associated amino acid mutations in the ORF1 of an HEV-1 strain Sar55 (AF444002) (Fig. 1A). Notably, we found that the exact positions of amino acid mutations

V27A, D29N, and H105R in the published case reports should be A27V, N30D, and R105H in HEV-1 strain Sar55. The 11 FHF-associated mutations located at different putative functional domains or regions in the HEV-1 ORF1 (26): A27V and N30D at the 5' end of ORF1; R105H and F179S at the Met; A317T at the Y domain; T735I at the HVR; L1110F and V1120I at the Hel; and F1439Y, C1483W, and N1530T at the RdRp (Fig. 1A). None of these FHF-associated mutations overlap with the ORF4 identified in HEV-1 (*SI Appendix, Fig. S1*) (14). In addition, we also mapped the 11 FHF-associated mutations to the ORF1 of an HEV-3 strain Kernow-C1 p6 (JQ679013) (designated p6 hereafter). However, the original amino acid residues in HEV-3 p6 at genomic positions 179, 317, 735, 1120, and 1439 are A (Ala), V (Val), I (Ile), I (Ile), and Y (Tyr), respectively, are different from the HEV-1 Sar55 strain (Fig. 1A).

Furthermore, we conducted comparative sequence analyses of each of the 11 FHF-associated mutations among the four major human-infecting HEV genotypes (82 genomes for HEV-1; 2 genomes for HEV-2; 644 genomes for HEV-3; and 225 genomes for HEV-4), which can reflect the epidemiological prevalence of these FHF-associated amino acid mutations at their respective positions (*SI Appendix, Table S1*). Since there are only two HEV-2 complete genomes available so far, HEV-2 was not presented or interpreted to avoid introducing potential sampling bias (Fig. 1B) (27). The amino acid residues at viral genomic positions 27, 30, 105, 1483, and 1530 are highly conserved among the three distinct HEV genotypes. Specifically, we found that the prevalence of A27, N30, R105, C1483, and N1530 is nearly 100% in HEV-1, and that the V27, D30, and H105 have a respective prevalence of only 4.88% (4/82), 3.66% (3/82), and 2.44% (2/82) within the HEV-1. In contrast, the amino acid residues at positions 179, 317, 735, 1110, 1120, and 1439 are relatively disordered in different HEV genotypes. At the amino acid positions 179 and 317, the F179 is the predominant (85.37%, 70/82) residue, and the A317 is more common (52.44%, 43/82) than T317 (45.12%, 37/82) in HEV-1; however, the prevalence of A179 and V317 is nearly 100% in HEV-3 and HEV-4. Similarly, T735 (57.32%, 47/82), L1110 (62.2%, 51/82), V1120 (54.88%, 45/82), and F1439 (85.37%, 70/82) possess a higher prevalence than their respective residues I735 (41.46%, 34/82), F1110 (37.8%, 31/82), I1120 (45.12%, 37/82), and Y1439 (14.63%, 12/82) in HEV-1, but these four positions have apparently different amino acid preference in HEV-3 and HEV-4, particularly Y1439 with a prevalence of 93.17% (600/644) in HEV-3 and 99.11% (223/225) in HEV-4 (*SI Appendix, Table S1*). Therefore, our comprehensive sequence analyses of the 11 FHF-associated mutations indicate that amino acid positions 27, 30, 105, 1483, and 1530 are evolutionarily conserved in the HEV genome, whereas positions 179, 317, 735, 1110, 1120, and 1439 can tolerate amino acid changes and preferentially hold different amino acid residues among the distinct HEV genotypes.

Two FHF-Associated Mutations in HEV-1, A317T and V1120I, Significantly Enhance HEV-1 Replication Efficiency *In Vitro*.

Recombinant virus replicons that encode indicator genes provide valuable tools for studying viral replication and sensitivity to small molecule inhibitors (17, 20, 28). Therefore, in this study we used an HEV-1 indicator replicon system to determine the effect of the 11 FHF-associated amino acid mutations on *in vitro* virus replication. The HEV-1 indicator replicon system was recently established based on the backbone of the HEV-1 Sar55 strain, and its partial N-terminal ORF2 sequence was replaced by a secreted version of the *Gaussia* luciferase (Gluc) gene (Fig. 2A) (29). The Sar55Gluc is replication

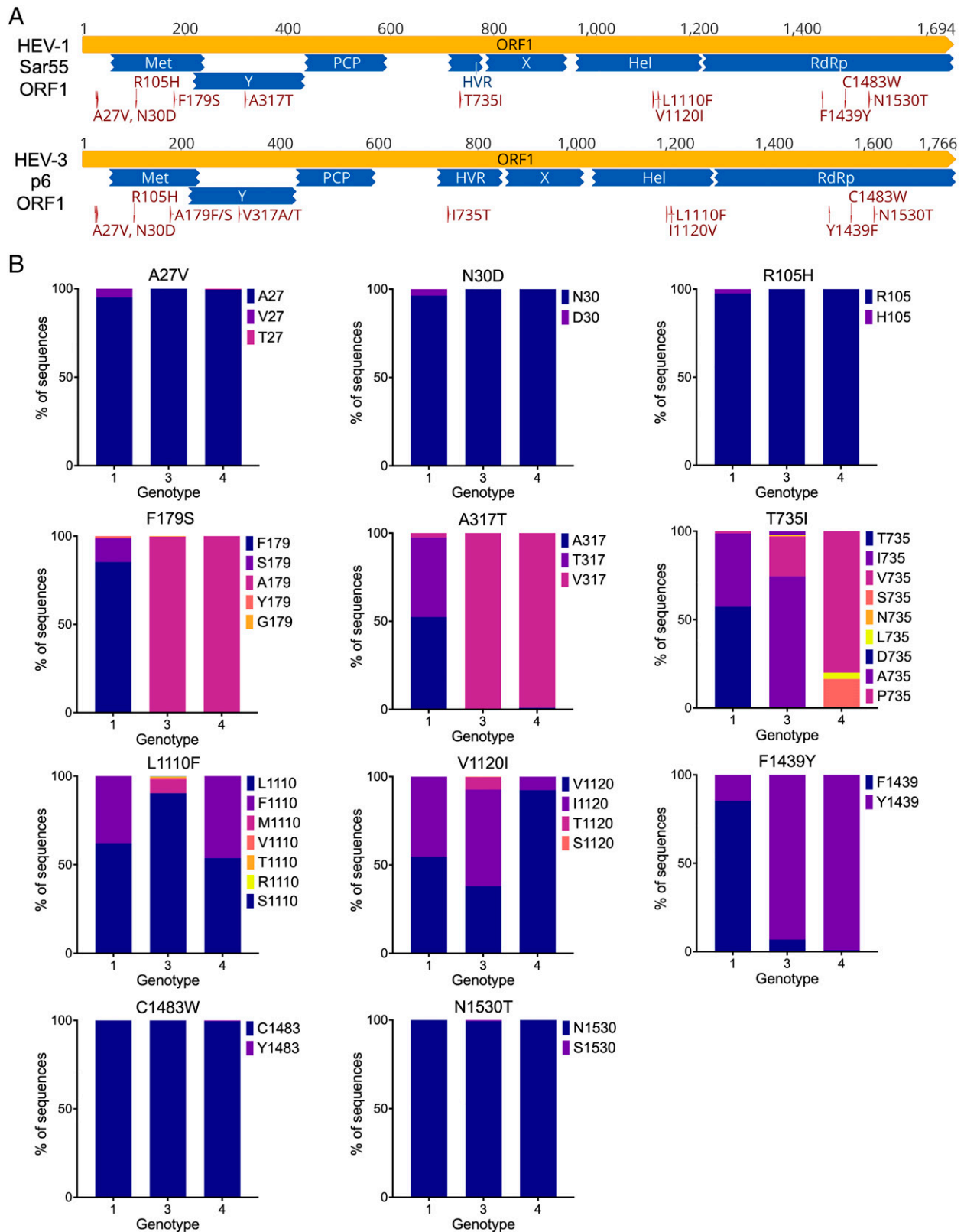


Fig. 1. Locations of the 11 FHF-associated mutations in the HEV ORF1 and epidemiological prevalence of the mutations at different amino acid positions in the three major human-infecting HEV genotypes. (A) Eleven FHF-associated HEV mutations from clinical case reports are identified and shown in the ORF1 of an HEV-1 strain Sar55 (AF444002) and an HEV-3 strain Kernow-C1 p6 (JQ679013). The putative functional domains within ORF1 are depicted. The ORF1 in amino acids is shown on the *Top*. (B) Prevalence of the 11 FHF-associated mutations at different amino acid positions among three major human-infecting HEV genotypes. HEV full-length genomes were retrieved (as of June 2022) from the GenBank database and aligned for comparative sequence analyses. The numbers of viral genomes analyzed for each genotype of HEV-1, HEV-3, and HEV-4 are 82, 644, and 225, respectively.

competent in several cultured cells and suitable for testing the HEV replication efficiency as demonstrated previously (29, 30). Measurement of daily Gluc activity for 12 d demonstrated that

Sar55Gluc is replication competent in Huh7-S10-3 liver cells, and that 7 d posttransfection would be sufficient to nearly reach peak luminescence (1.01×10^4 units) (Fig. 2B).

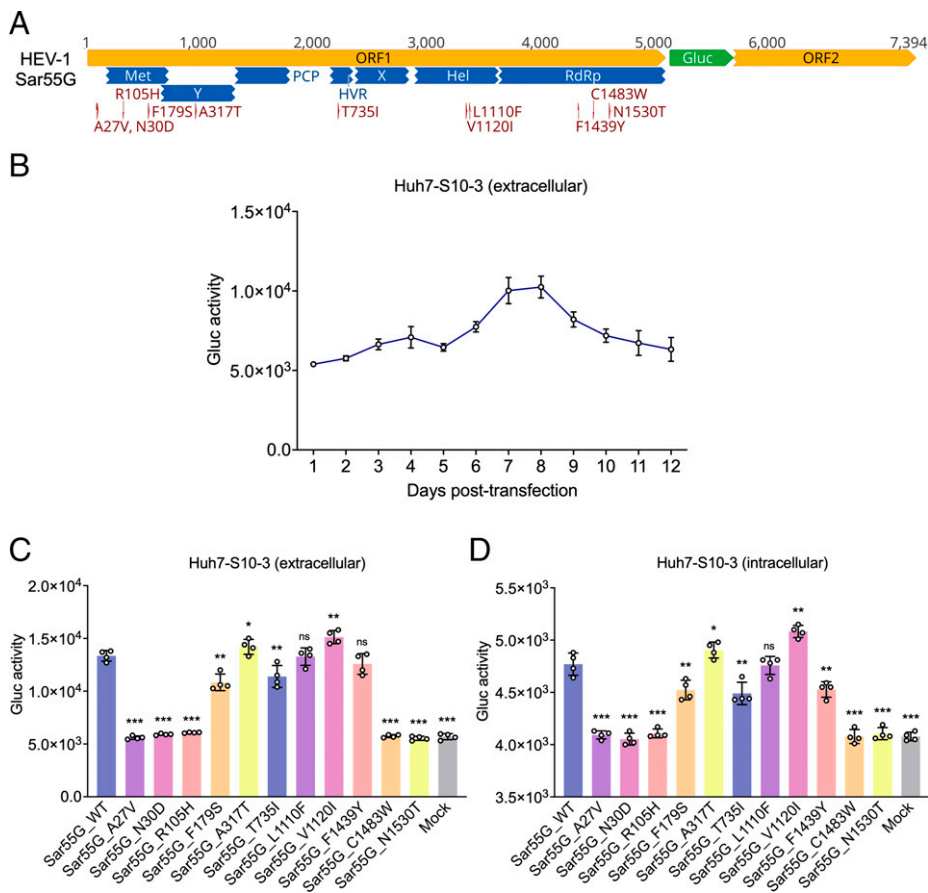


Fig. 2. Effect of FHF-associated mutations on the replication efficiency of an HEV-1 indicator replicon Sar55Gluc. (A) Schematic representation of the HEV-1 indicator replicon Sar55Gluc. The 11 FHF-associated mutations are shown. The Gluc gene is highlighted in green. The genome of the Sar55Gluc in nucleotide bases is shown on the *Top*. (B) Growth kinetics of wild-type Sar55Gluc as measured by Gluc expression activity. Cell culture media of Huh7-S10-3 cells were collected at different time points posttransfection of wild-type Sar55Gluc, and Gluc activity was monitored. Values represent means plus SDs (error bars) from four independent experiments ($n = 4$). (C and D) Comparative analyses of replication efficiency of Sar55Gluc wild type and mutants. At 7 d posttransfection with Sar55Gluc wild type and mutants, cell culture media (extracellular, C) and cell lysate (intracellular, D) of Huh7-S10-3 cells were harvested, and the Gluc activity was measured and compared. Values represent means plus SD (error bars) from four independent experiments ($n = 4$). Statistical significances were determined with one-way ANOVA. * $P < 0.05$, ** $P < 0.01$, and *** $P < 0.001$; ns, not statistically significant.

Subsequently, we generated 11 individual Sar55Gluc mutants (Sar55G_A27V, Sar55G_N30D, Sar55G_R105H, Sar55G_F179S, Sar55G_A317T, Sar55G_T735I, Sar55G_L1110F, Sar55G_V1120I, Sar55G_F1439Y, Sar55G_C1483W, and Sar55G_N1530T) each containing a single amino acid mutation, which corresponds to 1 of the 11 FHF-associated mutations. In each of the Sar55Gluc mutants, a single nucleotide was correctly substituted from wild-type Sar55Gluc (Sar55G_WT) using site-directed mutagenesis systems, according to the initial recorded nucleotide substitutions in HEV sequences of clinical FHF cases (*SI Appendix, Fig. S2*) (23–25). Next, the Gluc activity of Sar55G_WT and each of the 11 mutants were tested at 7 d posttransfection in the culture supernatant (extracellular) and cell lysates (intracellular) of Huh7-S10-3 liver cells (Fig. 2 C and D). Compared with Sar55G_WT, the Sar55G_A317T and Sar55G_V1120I mutants demonstrated significantly enhanced viral replication efficiency with 1.18-fold and 1.26-fold increases, respectively. On the contrary, the Sar55G_F179S and Sar55G_T735I significantly decreased viral replication, and the Sar55G_L1110F and Sar55G_F1439Y slightly decreased viral replication. However, the five additional mutants, Sar55G_A27V, Sar55G_N30D, Sar55G_R105H, Sar55G_C1483W, and Sar55G_N1530T, severely impaired viral replication to a level of mock transfection, which exhibited lethal phenotypes (Fig. 2C). The results derived from intracellular Gluc expression levels are highly consistent with those from extracellular levels despite the one log lower secreted luminescence (4.77×10^3 units) (Fig. 2D), indicating that the vast majority of the Gluc is expressed extracellularly.

To ensure the reproducibility of the results from the Sar55-Gluc indicator replicon screening, we also used the HEV-1 Sar55 infectious clone system for comparative mutational analysis to

further confirm the results from the Sar55Gluc indicator replicon system (31). Six selected FHF-associated mutations that yielded replication-enhanced or -reduced phenotypes in the Sar55Gluc system were individually introduced to the HEV-1 Sar55 infectious clone; thus, a total of six Sar55 single mutants (Sar55_F179S, Sar55_A317T, Sar55_T735I, Sar55_L1110F, Sar55_V1120I, and Sar55_F1439Y) were constructed (Fig. 3A). In vitro capped RNA transcripts from the wild-type Sar55 (Sar55_WT) and each of the six mutants were transfected to Huh7-S10-3 liver cells, and the transfected cells were stained with the anti-ORF2 antibody at 7 d posttransfection. HEV ORF2-positive foci were microscopically observed in Sar55_WT, Sar55_F179S, Sar55_A317T, Sar55_T735I, Sar55_L1110F, Sar55_V1120I, and Sar55_F1439Y (Fig. 3B). The amounts of virus in the media of transfected cells were quantified by measuring viral RNA loads with an HEV-specific RT-qPCR (32). We found that the Sar55_A317T and Sar55_V1120I replicated and/or assembled more efficiently than Sar55_WT, while mutants Sar55_F179S, Sar55_T735I, and Sar55_F1439Y significantly impaired viral replication. The Sar55_L1110F replicated at a slightly reduced level (Fig. 3C). Similar results were also obtained from the quantification of HEV-positive cells in the immunofluorescence assays (Fig. 3D). Overall, the results in determining the effect of FHF-associated amino acid mutations on viral replication using the HEV-1 Sar55 infectious clone system are consistent with the HEV-1 Sar55Gluc indicator replicon system. The introduction of amino acid mutations A317T and V1120I significantly increased HEV-1 Sar55 replication; conversely, mutations F179S, T735I, and F1439Y significantly decreased HEV-1 Sar55 replication; mutation L1110F slightly decreased HEV Sar55 replication.

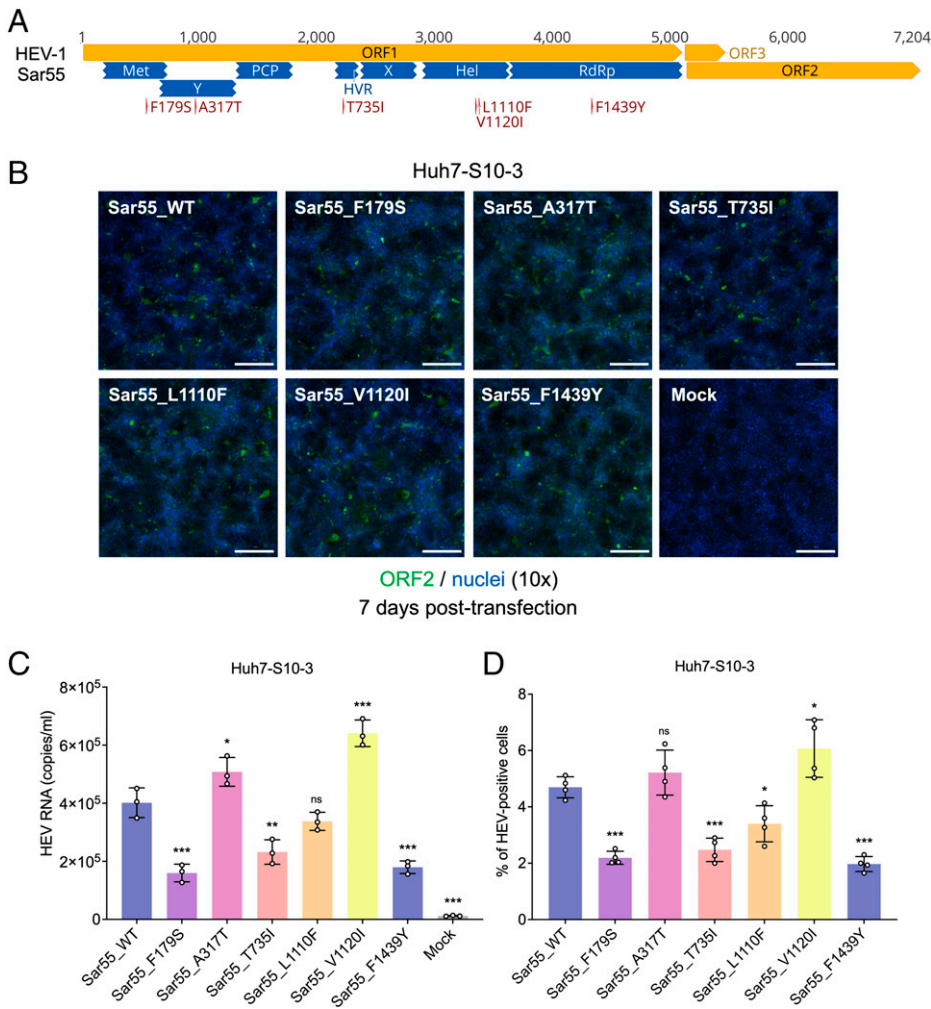


Fig. 3. Effect of selected FHF-associated mutations on *in vitro* replication of an HEV-1 infectious clone Sar55. (A) Schematic representation of the HEV-1 infectious clone Sar55. The six selected FHF-associated mutations are indicated. The genome of the HEV-1 Sar55 in nucleotide bases is shown on the *Top*. (B) Representative immunofluorescence staining of HEV-positive foci of Huh7-S10-3 cells at 7 d posttransfection of HEV-1 Sar55 wild type and mutants. HEV-positive foci are shown in green (anti-ORF2 polyclonal antibody derived from rabbit serum and goat anti-rabbit monoclonal antibody Alexa Fluor 488), and cell nuclei are shown in blue (DAPI). (Scale bar, 200 μ m.) (C) HEV RNA copy numbers were quantified by real-time RT-qPCR from the supernatant of Huh7-S10-3 cells at 7 d posttransfection of Sar55 wild type and mutants. Values represent means plus SDs (error bars) from three independent experiments ($n = 3$). (D) Number of HEV-positive cells at 7 d posttransfection of HEV-1 Sar55 wild type and mutants. Values represent means plus SD (error bars) from four independent experiments ($n = 4$). Statistical significances were determined with one-way ANOVA. * $P < 0.05$, ** $P < 0.01$, and *** $P < 0.001$; ns, not statistically significant.

The A317T/V1120I Double Mutant Significantly Enhances HEV-1 Sar55 Replication. Since we found that the single FHF-associated mutations, A317T and V1120I, significantly enhanced HEV Sar55 replication, it is important to examine the effect of the combination of these two mutations on viral fitness and infectivity. Therefore, we generated a Sar55G_A317T/V1120I double mutant using the HEV-1 Sar55Gluc replicon system as well as a Sar55_A317T/V1120I double mutant using the HEV-1 Sar55 infectious clone. The replication efficiency of the two double mutants was then compared with that of wild-type and single A317T or V1120I mutant Sar55Gluc and Sar55, respectively. We found that the Sar55G_A317T/V1120I double mutant replicated more efficiently than the Sar55G_A317T and Sar55G_V1120I single mutant with 1.16-fold and 1.23-fold increases, respectively (Fig. 4 *A* and *B*). Similar results were also obtained for the Sar55_A317T/V1120I double mutant using the Sar55 infectious clone. The viral loads and HEV-positive cells of the Sar55_A317T/V1120I double mutant were significantly higher than those of the Sar55_WT, Sar55_A317T, and Sar55_V1120I in transfected Huh7-S10-3 liver cells (Fig. 4 *C–E*). Taken together, the results strongly indicate that two unique FHF-associated mutations in combination significantly enhanced HEV-1 replication compared to each of the single mutations alone.

The A317T and V1120I Mutations Are Associated with HEV Outbreaks and Severe Diseases. We showed that the two FHF-associated mutations (A317T and V1120I) each significantly enhanced virus replication efficiency, and that the combinational

double mutant of A317T and V1120I significantly enhanced viral replication compared to each of the single mutation. Our *in vitro* results regarding the potential role of these two mutations in viral pathogenicity and FHF are further corroborated by a recent study in which 21 HEV-1 whole-genome sequences were obtained from HEV IgM-positive patients from 2013 to 2015 in Bangladesh. These tightly clustered HEV strains were associated with HEV outbreaks and FHF/ALF (33). Remarkably, we found that the two unique amino acid mutations (A317T and V1120I) simultaneously occurred in 100% of all 21 HEV-1 genomes derived from FHF patients during HEV outbreaks from 2013 to 2015 in Bangladesh (Fig. 4*F*). Since we demonstrated in this study that A317T and V1120I significantly enhanced HEV-1 replication *in vitro*, it is likely that these two unique mutations play an important role in the rapid viral replication and severe liver disease in HEV-infected FHF patients. Although the L1110F mutation also appeared in 80.9% (17/21) of HEV outbreak strains (Fig. 4*F*), this mutation did not significantly affect viral replication efficiency compared with the wild-type Sar55 in our *in vitro* results. It should be noted that other FHF-associated mutations, including A27V, N30D, R105H, F179S, C1483W, N1530T, and F1439Y, which negatively impacted HEV-1 replication *in vitro*, did not occur in any of these HEV-1 genomes. Intriguingly, the T735I mutation, which significantly reduced HEV-1 replication *in vitro*, appeared in all of these HEV-1 genomes; however, the potential functional role of T735I in HEV-associated FHF remains to be determined.

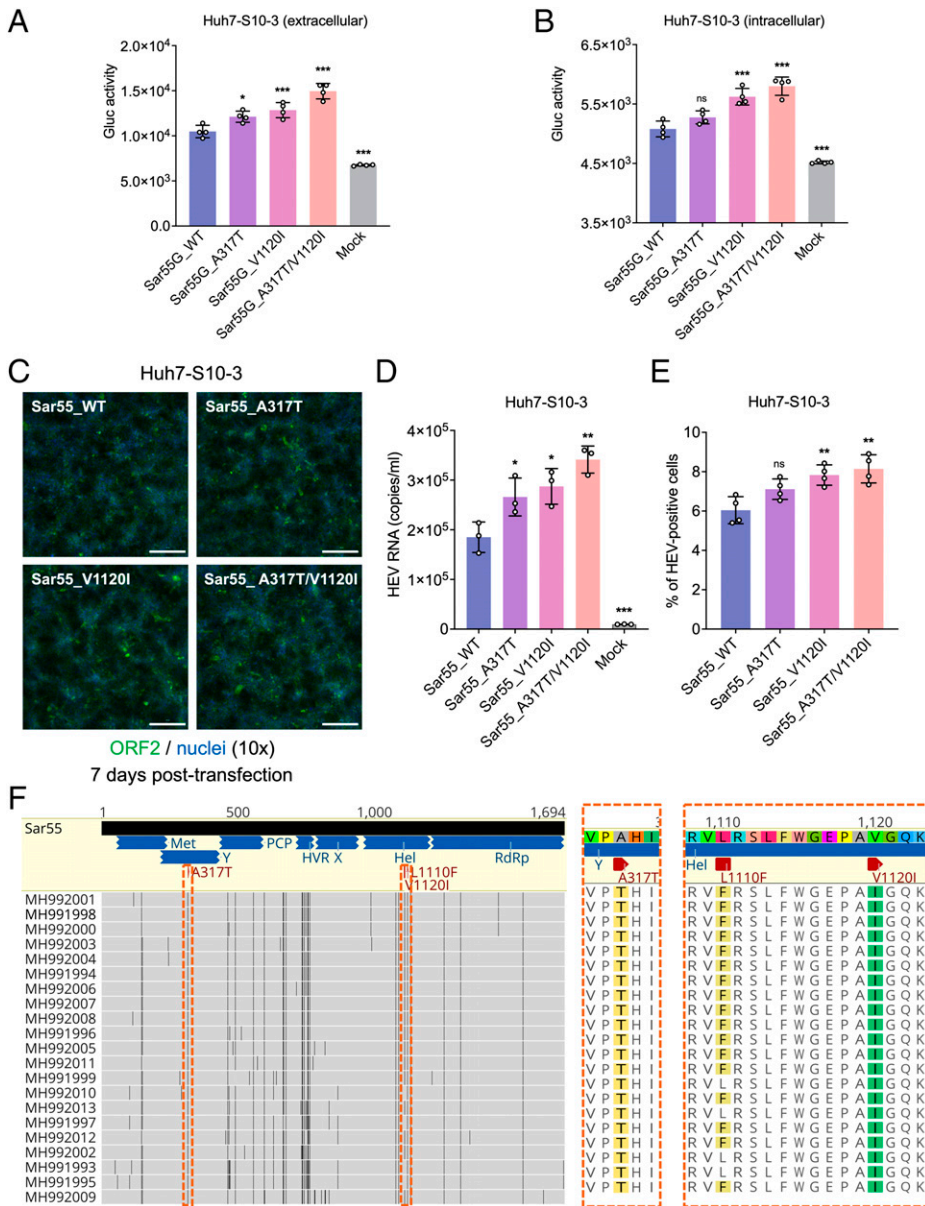


Fig. 4. The A317T/V1120I double mutant greatly enhances HEV-1 Sar55 replication. (A and B) Comparative analyses of replication efficiency of HEV-1 wild-type Sar55Gluc and mutant Sar55Gluc with a single amino acid mutation A317T or V1120I, or double mutations A317T/V1120I. At 7 d posttransfection of Sar55Gluc wild type and mutants, cell culture media (extracellular, A) and cell lysate (intracellular, B) of Huh7-S10-3 cells were harvested, and the Gluc activity was measured and compared. Values represent means plus SDs (error bars) from four independent experiments ($n = 4$). (C) Representative immunofluorescence staining of HEV-positive foci of Huh7-S10-3 cells at 7 d posttransfection of HEV-1 Sar55 wild type and mutants. HEV-positive foci are shown in green, and cell nuclei are shown in blue. (Scale bar, 200 μm .) (D) HEV RNA copy numbers were quantified by real-time RT-qPCR from the supernatant of Huh7-S10-3 cells at 7 d posttransfection of HEV-1 Sar55 wild type and mutants. Values represent means plus SD (error bars) from three independent experiments ($n = 3$). (E) Number of HEV-positive cells at 7 d posttransfection of HEV-1 Sar55 wild type and mutants. Values represent means plus SD (error bars) from four independent experiments ($n = 4$). Statistical significances were determined with one-way ANOVA. * $P < 0.05$, ** $P < 0.01$, and *** $P < 0.001$; ns, not statistically significantly. (F) Amino acid sequence alignment of the ORF1 of HEV-1 Sar55 and endemic strains from Bangladesh. The amino acid mutations A317T, L1110F, and V1120I, are zoomed in and indicated on the Right.

Effect of FHF-Associated Mutations on In Vitro Replication and Infectivity of an HEV-3 Strain (Kernow-C1 p6). HEV FHF cases are associated almost exclusively with HEV-1 infection in clinical case reports (2, 3), and therefore the FHF-associated mutations are supposedly restricted to HEV-1 and are not expected to enhance virus replication in other HEV genotypes. To further confirm that the enhanced virus replication of the two FHF-associated mutations A317T and V1120I are phenotypically specific to HEV-1, we determined the effect of the FHF-associated mutations on the replication efficiency of an HEV-3 strain (Kernow-C1 p6) by employing the well-established Kernow-C1 p6 indicator replicon and infectious clone systems (34, 35). Since the HEV-3 Kernow-C1 p6 is well adapted to grow in the human hepatocellular carcinoma cells and can also efficiently replicate in several other cultured cells (34, 35), this HEV-3 strain has been extensively studied, and the infectious cDNA clone p6 and indicator replicon p6Gluc systems have been established and widely used in various HEV functional, mutational, and structural studies (17, 18, 20, 28–30).

Like HEV-1 Sar55Gluc, the HEV-3 p6Gluc replicon also contains a secreted Gluc gene in replacement of a partial HEV

ORF2 sequence (Fig. 5A). The growth kinetics of p6Gluc showed that extracellular luminescence activity peaks at 7 d posttransfection with $\sim 2.6 \times 10^6$ Gluc activity units (Fig. 5B). Subsequently, we generated a panel of HEV-3 p6Gluc mutants with each single altered FHF-associated amino acid mutation. Because the original amino acid residues in HEV-3 p6 at genomic positions 179 and 317 are A (Ala) and V (Val), respectively, we thence mutated A179 to 179F and 179S; likewise, V317 was mutated to 317A and 317T. Additionally, a G1634R mutation was included to serve as a “relevant” positive control, since it has been reported that the G1634R mutation significantly promoted the HEV-3 replication (17, 20, 28). Therefore, a panel of 14 HEV-3 p6Gluc mutants was successfully constructed, including p6G_A27V, p6G_N30D, p6G_R105H, p6G_A179F, p6G_A179S, p6G_V317A, p6G_V317T, p6G_I735T, p6G_L1110F, p6G_I1120V, p6G_Y1439F, p6G_C1483W, p6G_N1530T, and p6G_G1634R, each mutant with substitution of one or two nucleotides in wild-type p6Gluc (p6G_WT) (SI Appendix, Fig. S3). Comparisons of Gluc activity from the culture supernatant (extracellular) and cell lysates (intracellular) of Huh7-S10-3 liver cells at 7 d posttransfection revealed that all FHF-associated

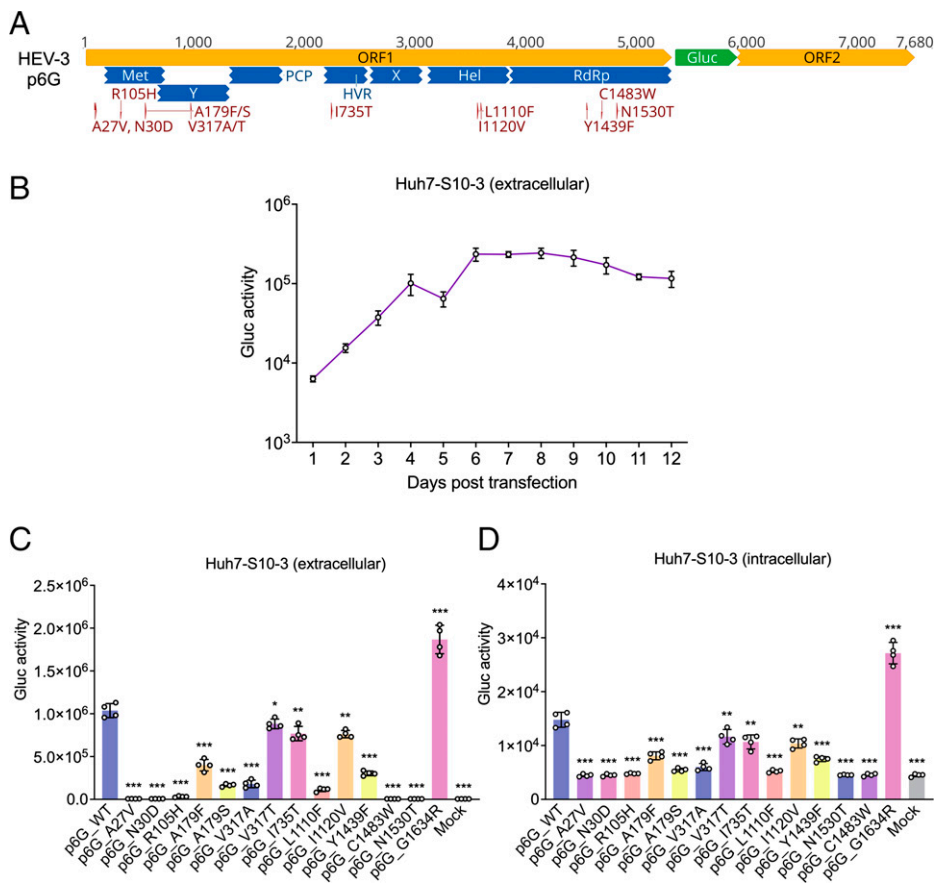


Fig. 5. Effect of FHF-associated mutations on replication efficiency of an HEV-3 Kernow-C1 p6Gluc indicator replicon. (A) Schematic representation of the HEV-3 indicator replicon p6Gluc. The 11 FHF-associated mutations are indicated. The Gluc gene is highlighted in green. The genome of the p6Gluc in nucleotide bases is shown on the *Top*. (B) Growth kinetics of wild-type p6Gluc as measured by Gluc expression activity. Culture media of Huh7-S10-3 cells were collected at different time points posttransfection of wild-type Sar55Gluc, and the Gluc activity was monitored. Values represent means plus SDs (error bars) from four independent experiments ($n = 4$). (C and D) Comparative analyses of replication ability of HEV-3 p6Gluc wild type and mutants. At 7 d posttransfection of p6Gluc wild type and mutants, cell culture media (extracellular, C) and cell lysate (intracellular, D) of Huh7-S10-3 cells were harvested, and the Gluc activity was measured and compared. Values represent means plus SD (error bars) from four independent experiments ($n = 4$). Statistical significances were determined with one-way ANOVA. * $P < 0.05$, ** $P < 0.01$, and *** $P < 0.001$.

mutations impaired HEV-3 viral replication to a large extent when compared with p6G_WT (Fig. 5 C and D). Of note, similar to the results from HEV-1 Sar55Gluc, we also found that the mutations A27V, N30D, R105H, C1483W, and N1530T abrogated HEV-3 viral replication, further suggesting that these five mutations are lethal to HEV replication. Expectedly, the G1634R mutation that served as a relevant positive control significantly enhanced viral replication with 1.84-fold extracellular and 1.80-fold intracellular increases, respectively (Fig. 5 C and D), as extensively documented in other HEV studies (17, 18, 20, 28).

To further confirm the results from the HEV-3 p6Gluc replicon system, we used the HEV-3 p6 infectious clone backbone to construct nine selected HEV-3 p6 mutants, including p6_A179F, p6_A179S, p6_V317A, p6_V317T, p6_I735T, p6_L1110F, p6_I1120V, p6_Y1439F, and p6_G1634R (Fig. 6A). Because of the more efficient replication capacity of the wild-type HEV-3 p6 (p6_WT) in cultured cells, HEV ORF2-positive foci could be readily observed in transfected Huh7-S10-3 liver cells; however, there are obviously fewer HEV ORF2-positive foci in p6_A179S, p6_V317A, and p6_L1110F mutants compared with that in p6_WT (Fig. 6B). HEV-specific RT-qPCR quantification of viral RNA loads in the media of transfected cells and Western blotting analysis of HEV ORF2 protein in the lysates of Huh7-S10-3 cells from HEV-3 p6_WT and selected mutants demonstrated that the introduction of single A179F, V317T, I745T, I1120V, and Y1439F mutations decreased HEV-3 viral replication and capsid protein expression. Conversely, the relevant positive control G1634R mutation increased HEV-3 viral replication and capsid protein expression (Fig. 6 C and D).

Moreover, we also assessed and compared the infectivity of p6_WT with various other HEV-3 p6 mutants. The HEV focus-forming infectivity assay is adapted from a recently established robust cell culture HEV infection system based on the HEV-3 p6 strain and human hepatoma cell line HepG2/C3A (28) (*SI Appendix, Fig. S4*). The HepG2/C3A liver cells are readily infected by virus stocks harvested from five consecutive passages of HEV-3 p6-transfected Huh7-S10-3 liver cells, although the intracellular nonenveloped HEV (neHEV) p6 was more infectious (9.27×10^4 FFU/mL) than quasi-enveloped (eHEV) HEV-3 p6 (7.12×10^5 FFU/mL) (*SI Appendix, Fig. S4 A and B*), which is consistent with the results from previous studies (28, 36). In focus-forming infectivity assays, the p6_WT HEV infected more HepG2/C3A liver cells with significantly higher viral titers (1.63×10^3 FFU/mL) than those of p6 mutants with a single FHF-associated mutation; on the contrary, the RBV treatment failure-associated HEV-3 mutation G1634R, which is used as a relevant positive control in this study, significantly enhanced viral replication ability and infectivity (2.58×10^3 FFU/mL) (Fig. 7 A and B) (20). Additionally, we also transfected HepG2/C3A liver cells with wild-type and mutant p6Gluc indicator replicons and found that the trend of luminescence activity levels of different p6Gluc mutants in HepG2/C3A cells was consistent with that in Huh7-S10-3 cells, albeit with much lower Gluc activity (7.29×10^3 units) (Fig. 7C). Taken together, these data strongly indicate that the introduction of FHF-associated mutations to HEV-3 Kernow-C1 p6 significantly decreased the replication ability and infectivity of HEV-3, suggesting that the enhanced viral replication of the two FHF-associated mutations (A317T and V1120I) identified from this study is likely phenotypically specific to HEV-1.

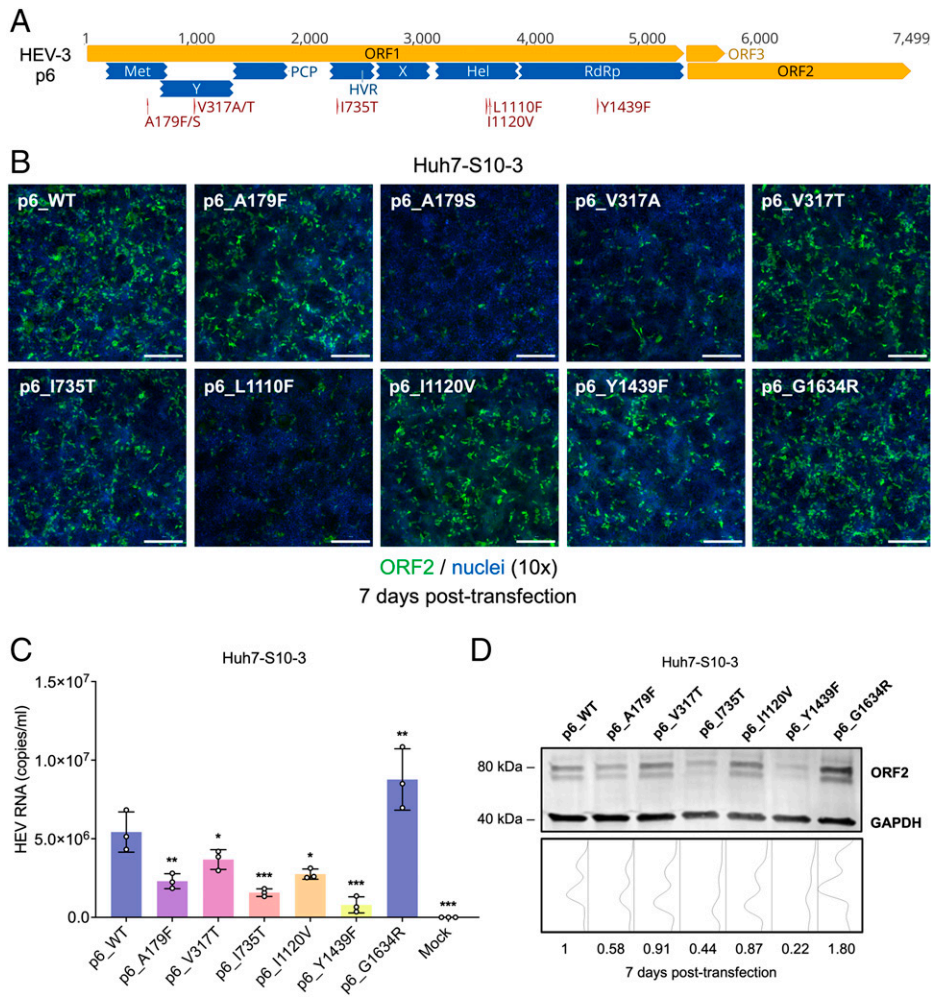


Fig. 6. Effect of selected FHF-associated mutations on in vitro replication of an HEV-3 infectious clone p6. (A) Schematic representation of the HEV-3 infectious clone p6. The six selected FHF-associated mutations are indicated. The genome of the HEV-3 p6 in nucleotide bases is shown on the *Top*. (B) Representative immunofluorescence staining of HEV-positive foci of Huh7-S10-3 cells at 7 d posttransfection of HEV-3 p6 wild type and mutants. HEV-positive foci are shown in green, and cell nuclei are shown in blue. (Scale bar, 200 μ m.) (C) HEV RNA copy numbers were quantified by real-time RT-qPCR from the supernatant of Huh7-S10-3 cells at 7 d posttransfection of p6 wild type and selected p6 mutants. Values represent means plus SDs (error bars) from three independent experiments ($n = 3$). Statistical significances were determined with one-way ANOVA. * $P < 0.05$, ** $P < 0.01$, and *** $P < 0.001$; ns, not statistically significant. (D) Western blot analysis of Huh7-S10-3 cells at 7 d posttransfection of p6 wild type and selected p6 mutants. Cell lysates were harvested for detection of HEV ORF2 capsid protein using an anti-HEV ORF2 antibody. GAPDH was served as a sample processing control. The ratios of HEV ORF2 expression from different p6 mutants are indicated at the *Bottom*.

RBV Treatment Significantly Inhibits the Replication Efficiency of HEV-1 Sar55 and HEV-3 p6 with FHF-Associated Mutations.

FHF cases occur in pregnant women infected with HEV-1, which require antiviral therapy (2, 3); however, there are currently no direct-acting and nonteratogenic treatment options available against HEV (1). Nonetheless, considering the potent antiviral effects of RBV against HEV, it is important to determine whether RBV treatment is still effective against HEV mutants with FHF-associated mutations in other HEV-infected nonpregnant females and males. Recently, several amino acid changes in the HEV-3 RdRp have reportedly occurred during RBV monotherapy in CHE patients, including Y1320H, K1383N, D1384G, K1398R, V1479I, Y1587F, and G1634R (17–20). Notably, the K1383N mutation significantly altered viral fitness as well as RBV sensitivity and may play a crucial role in the RBV treatment failure in clinical cases (17, 21). It is reported that the calculated 50% effective concentration of RBV is 5.1 μ M for both wild-type HEV-3 p6 and the HEV-3 p6 G1634R mutant (20).

To assess the impact of FHF-associated mutations on HEV sensitivity to RBV, we added either 10 μ M or 100 μ M RBV to Huh7-S10-3 cells transfected with wild-type and mutant HEV indicator replicons, and cells with absence of RBV served as controls. The results from luminescence-based antiviral assays showed that administration of 10 μ M RBV significantly inhibited the replication efficiency of both HEV-1 Sar55 and HEV-3 p6 containing the FHF-associated mutations, and administration of 100 μ M RBV reduced the luminescence activity to

mock levels (Fig. 8 A and B). No Sar55Gluc or p6Gluc mutants yielded an RBV-resistant phenotype. Thus, the FHF-associated mutations did not alter RBV susceptibility, suggesting that RBV treatment of HEV-1-associated FHF cases, remains a viable option. However, due to the risk of embryocidal and teratogenic effects, RBV is not recommended for use in pregnant women and the development of new HEV-specific antivirals is urgently needed (2, 3, 5).

Physicochemical and Structural Analyses of FHF-Associated Mutations in the HEV-1 Genome.

Based on our comprehensive experimental results described above, the influence of FHF-associated mutations on in vitro replication efficiency of the HEV-1 strain Sar55 is schematically presented and interpreted in *SI Appendix, Fig. S5*. Given that the A27V and N30D mutations locate at the functional *Cis*-acting RNA element (CARE) at the 5' end of HEV ORF1 (*SI Appendix, Fig. S5A*), this CARE is highly conserved across different HEV genotypes (*SI Appendix, Fig. S6*) (30). It seems reasonable to speculate that a single nucleotide substitution in this region can greatly affect the secondary structure of HEV RNA, which would explain the abolishment of viral replication of A27V and N30D mutations for both HEV-1 Sar55 and HEV-3 p6 (Figs. 2 and 5). The T735I mutation is located in the HEV HVR, which is also known as the polyproline-rich region (PPR), and is vulnerable to substitutions, insertions, deletions, and duplications (37). We showed that this position is highly heterogenic in different HEV genotypes, particularly in HEV-4 (Fig. 2B). The R105H and

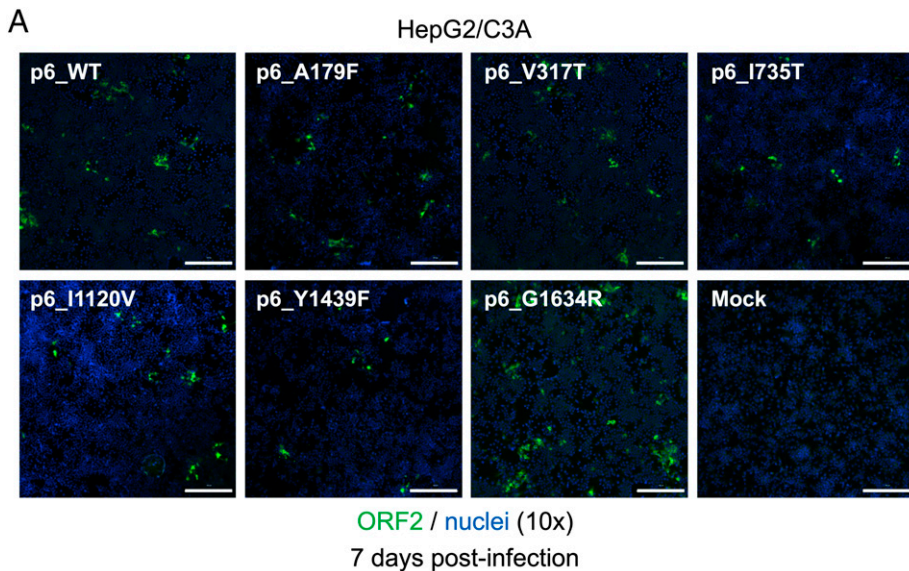
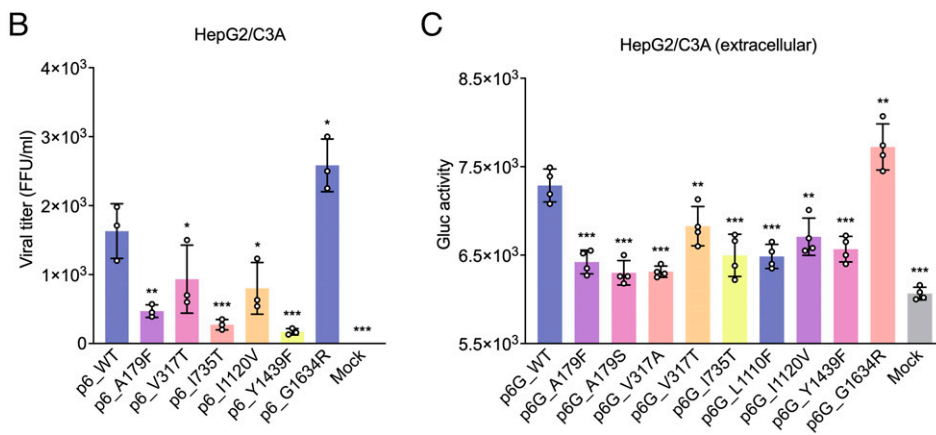


Fig. 7. Effect of selected FHF-associated mutations on in vitro replication and infectivity of HEV-3 p6 and p6Gluc in HepG2/C3A cells. (A) Representative immunofluorescence staining of HEV-positive foci of HepG2/C3A cells at 7 d postinfection of HEV-3 p6 wild type and mutants. The inocula of wild-type and mutant viruses were produced from the supernatant of Huh7-S10-3 cells transfected with p6 wild type and mutants, respectively. HEV-positive foci are shown in green, and cell nuclei are shown in blue. (Scale bar, 200 μ m.) (B) Infectivity of HEV-3 p6 wild-type and selected p6 mutant virions were compared and recorded by microscopically counting HEV-positive foci. Values represent means plus SDs (error bars) from three independent experiments ($n = 3$). (C) Comparisons of replication ability of p6G wild type and mutants in HepG2/C3A. At 7 d posttransfection of p6Gluc wild type and mutants, cell culture media (extracellular) of HepG2/C3A cells were harvested, and the Gluc activity was measured and compared. Values represent means plus SD (error bars) from four independent experiments ($n = 4$). Statistical significances were determined with one-way ANOVA. * $P < 0.05$, ** $P < 0.01$, and *** $P < 0.001$.



F179S mutations locate in the functional Met, and the A317T mutation locates in the putative Y domain (*SI Appendix, Fig. S5 B and C*). It has been suggested that the Y domain is an extension of the Met and is indispensable for viral replication and virion infectivity (38). Notably, the R105H is in the Met Ia2 motif. Therefore, the R105H mutation may alter the structural conformations of the Met, which can result in the abrogation of viral replication, even though both R (Arg) and H (His) are positively charged amino acids. The substitution of hydrophobic amino acid residue F (Phe) to polar uncharged S (Ser) at position 179 in the Met significantly decreased HEV-1 Sar55 replication; conversely, the substitution of hydrophobic amino acid residue A (Ala) to polar uncharged T (Thr) at position 317 in the Y domain significantly increased HEV-1 Sar55 replication. To what extent the biochemical properties of these unique amino acids affect HEV replication efficiency is still to be determined.

The L1110F and V1120I mutations locate between the IV and V motifs of the functional Hel (*SI Appendix, Fig. S5D*). Although the four amino acid residues of L (Leu), F (Phe), V (Val), I (Ile) have similar hydrophobic properties, the L1110F mutation displayed a replication-reduced phenotype, but the V1120I mutation exhibited a replication-enhanced phenotype in HEV-1 mutational analyses (Figs. 2 and 3). Lastly, the F1439Y, C1483W, and N1530T mutations are located in the HEV functional RdRp, which is crucial for viral replication and transcription (*SI Appendix, Fig. S5E*) (13). Unique HEV-3 RdRp mutations in patients chronically infected with HEV

have reportedly altered viral virulence and antiviral sensitivity (17, 20). Although the F1439Y mutation is in the RdRp structural III motif, our in vitro results showed that this position could bear amino acid changes, at least for the two amino acids, F (Phe) and Y (Tyr). Indeed, as shown in our sequence analyses, most HEV-1 strains prefer F1439, whereas the vast majority of HEV-3 and HEV-4 strains favor Y1439 (Fig. 1B). Notably, either the F1439Y mutation in HEV-1 Sar55 or the Y1439F mutation in HEV-3 p6 significantly decreased viral replication. Hypothetically, the different preference of F1439 or Y1439 is likely due to the distinct evolutionary process of different HEV genotypes (12). However, the C1483W and N1530T mutations seemed to be fatal for both HEV-1 Sar55 and HEV-3 p6 in our in vitro experimental analysis (Figs. 2 and 5). It is also to be noted that the W1483 and T1530 did not exist in any of the currently available HEV strains (Fig. 1B). Thus, whether the FHF-associated HEV-1 RdRp mutations C1483W and N1530T play a role, if any, in HEV pathogenesis remains unknown.

Collectively, we systematically investigated 11 clinically reported FHF-associated HEV-1 mutations in silico and in vitro using relevant HEV-1 replicon and infectious clone systems. Importantly, we demonstrated that the FHF-associated A317T and V1120I mutations increased HEV-1 replication, and that the enhanced viral fitness and replication efficiency of the double mutant may contribute to the increased viremia and poor clinical outcome such as FHF in HEV-1-infected patients.

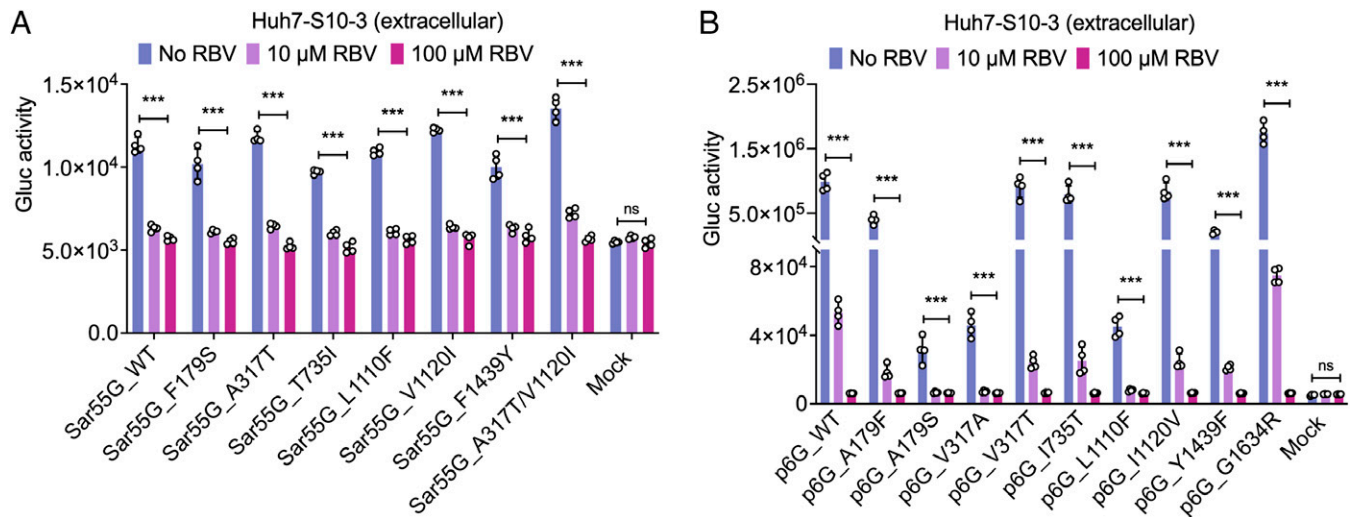


Fig. 8. Impact of RBV on in vitro replication efficiency of HEV-1 Sar55Gluc and HEV-3 Kernow-C1 p6Gluc indicator replicons with FHF-associated mutations. (A) Comparative analyses of RBV sensitivity of HEV-1 Sar55Gluc wild type and mutants. Huh7-S10-3 cells were cultured without RBV or with 10 μ M RBV or 100 μ M RBV. At 7 d posttransfection of Sar55Gluc wild type and mutants, cell culture media (extracellular) of Huh7-S10-3 cells were collected, and the Gluc activity was measured and compared. (B) Comparative analyses of RBV sensitivity of HEV-3 p6Gluc wild type and mutants. Huh7-S10-3 cells were cultured without RBV or with 10 μ M RBV or 100 μ M RBV. At 7 d posttransfection of p6Gluc wild type and mutants, cell culture media (extracellular) of Huh7-S10-3 cells were harvested, and the Gluc activity was measured and compared. Values represent means plus SDs (error bars) from four independent experiments ($n = 4$). Statistical significances were determined with one-way ANOVA. *** $P < 0.001$; ns, not statistically significant.

Discussion

A unique feature of HEV infection is the high incidence of FHF with significant mortality in pregnant women, although FHF also occurs in other HEV-infected nonpregnant females and males (2, 3). For example, it was reported that FHF developed in 22.2% (8/36) of pregnant women with viral hepatitis, compared to 2.8% (3/107) of men with HEV infection in India (39). Another study from India reported a prevalence of 34.6% (44/127) and 11.6% (17/146) of FHF in pregnant and nonpregnant women, respectively. Notably, the mortality rate (56.8%, 25/44) was extremely high among HEV-infected FHF cases during the third trimester of pregnancy (40). In Pakistan, of the 53 HEV-infected pregnant patients, 20 (37.7%) developed FHF with eight mortalities (case fatality rate 15%) (41). HEV-1 is almost exclusively responsible for FHF in developing countries; in contrast, HEV-3 and HEV-4 are unlikely to cause FHF in pregnant women (3). The underlying molecular mechanisms of severe liver injury of HEV-1 infection in pregnant women remain largely unknown. Both host and viral factors, such as altered hormone levels and immunologic responses and HEV heterogeneity, could have contributed to the severity of the liver diseases in infected pregnant women (21, 42, 43). Notably, levels of pregnancy-associated hormones, including estrogen, progesterone, and β -human chorionic gonadotrophin, were significantly higher in HEV-positive pregnant women compared with those of HEV-negative pregnant women or HEV-positive nonpregnant women (44). Indeed, we have recently shown that progesterone, which is an essential hormone for the maintenance of pregnancy, increased HEV-3 replication in human liver cells (45). Additionally, heightened immune responses may also link to the onset of liver damages as higher anti-HEV IgM and IgG titers and more frequent HEV-specific CD4⁺ and CD8⁺ T cells have been observed in HEV-infected patients with FHF than those with self-limiting conditions (46). Thus far, nearly a dozen amino acid changes in the HEV genome have been reportedly linked to patients with FHF in clinical cases, but experimental confirmation of the role of these amino acid changes in FHF is still lacking

(23–25), largely due to the lack of an efficient cell culture and suitable animal model for HEV-1.

By utilizing the HEV-1 replicon and infectious clone, we determined the functional impact of the 11 FHF-associated mutations on virus replication and infectivity. We demonstrated that most of the mutations actually impaired HEV-1 replication efficiency because of distinct physicochemical and structural features of amino acid residues; however, 2 of the 11 FHF-associated mutations, the A317T mutation in the Y domain and the V1120I mutation in Hel, significantly enhanced HEV-1 replication efficiency in cultured liver cells (Figs. 2 and 3). Importantly, these same two unique mutations simultaneously occurred in 100% of 21 tightly clustered HEV-1 strains detected in outbreaks from Bangladesh, which are associated with FHF in patients (33). Furthermore, we demonstrated that a combinational mutant containing A317T/I1120I double mutations significantly increased HEV replication efficiency than either mutation alone (Fig. 4), indicating that these two HEV-1 mutations may contribute to the rapid viral spread and severe diseases in HEV-infected patients. A previous study from India indicated that V1120I greatly reduced the level of HEV-1 replication (47). They utilized the Sar55 indicator replicon containing a *Renilla* luciferase (Rluc) gene, which is less stable and 1,000-fold less sensitive than Gluc reporter system and is only secreted intracellularly (48, 49). Our results from the Gluc assays were further validated using HEV-specific RT-PCR (Figs. 2 and 3). The other four mutations (F179S, T735I, L1110F, and F1439Y) decreased HEV-1 replication to some degree. How these two FHF-associated mutations cause enhanced virus replication and severe diseases remains unknown, but they may interact with unknown host factors to modulate virus replication efficiency and host immune responses (42, 50). A major limitation in this study is the low replication efficiency of HEV-1 Sar55 in cell cultures. However, the HEV-1 replicon and infectious clone system we used in this study are the best systems currently available for studying HEV-1 replication.

HEV genotype-associated phenotypical differences in disease severity (5, 43) and HEV-3 mutations in altered viral fitness and antiviral sensitivity have been extensively studied (17–20).

In contrast, a previous statistical analysis with small numbers of virus genomes has suggested that HEV genotypes, variants, or specific substitutions appeared to be not responsible for FHF, and therefore the role of HEV-1 FHF mutations in HEV pathogenesis was questionable (51). In this study, we found that the prevalence of amino acid residues at viral genomic positions 179, 317, 735, 1110, 1120, and 1439 is significantly different across distinct HEV genotypes (Fig. 1), and that amino acid substitutions in these positions significantly decreased HEV-3 replication (Figs. 5–7), which is reminiscent of the unique G1634R mutation that promoted the fitness of HEV-3 but not HEV-1 (20). Considering the distinct host range, geographical distributions, infection patterns, and clinical courses between HEV-1 and HEV-3, the amino acid preference for different HEV genotypes is reasonable (9, 11). Importantly, there is no evidence of a correlation between FHF and HEV-3 infection (2, 3). Finally, the remaining five FHF-associated mutations (A27V, N30D, R105H, C1483W, and N1530T) drastically decreased viral replication of both HEV-1 and HEV-3 and seemed to be lethal mutations, which is likely due to altered structural conformations in the genome (*SI Appendix, Fig. S5*). Indeed, the amino acids A27, N30, R105, C1483, and N1530 are highly conserved across different HEV genotypes, while the V27, D30, H105, W1483, and T1530 were only reported in two consecutive studies from the same research group in India (24, 25); thus, independent confirmation is still lacking for the occurrence of these FHF-associated mutations. Nonetheless, the clinical relevance of these FHF-associated mutations should not be completely ignored, given that the recently identified unique HEV-3 K1383N mutation almost abrogated viral replication but yet still played an important role in the anti-RBV resistance (17).

Significant progress has been made recently in the propagation of certain HEV strains in different cell lines (16). In this study, we employed both Huh7-S10-3 and HepG2/C3A cell culture models along with reverse genetic approaches to determine the effect of FHF-associated mutations on HEV replication efficiency and infectivity. Importantly, the use of both HEV-1 Sar55 and HEV-3 p6 infectious clone and indicator replicon systems greatly ensured the reproducibility of our results. Nonetheless, the HEV replication is still limited with low infectious titers in cultured cells, particularly for HEV-1, which hampers the comparative analysis of infectivity of some viral mutants. On the other hand, it is not neglectable that, apart from the identified FHF-associated amino acids, there is also a considerable sequence divergence in other viral genomic regions between the HEV variants derived from FHF patients and the HEV-1 Sar55 strain. For example, different replication efficacies have been noticed between HEV-3 p6 and HEV-3 p6 chimeric constructs with HEV ORF1 sequences from patients, indicating that other viral elements may also contribute to HEV virulence (17). Therefore, the effect of FHF-associated mutants on HEV-1 Sar55 might not be entirely translatable to endemic HEV-1 strains. An animal study in HEV-1 susceptible pregnant nonhuman primates, which is beyond the scope of the present study, is required to more definitively determine whether the two identified FHF-associated mutations truly contribute to FHF.

Currently, treatment options for hepatitis E, including pegylated IFN and RBV, are very limited (5). RBV monotherapy is promising in treating HEV infections, although it can cause significant side effects (5). Moreover, RBV induces viral mutagenesis and increases HEV heterogeneity, and treatment failure has been documented due to the emergence of RBV-resistant

mutations, whose impact on HEV pathogenicity and antiviral susceptibility are poorly understood due to the lack of a tractable chronic HEV infection animal model (5, 6, 17, 18, 20). Since HEV-1-associated FHF cases do require antiviral therapy, it is important to determine whether the FHF-associated mutations affect RBV sensitivity. Our results demonstrated that RBV is highly effective in inhibiting the virus replication of both HEV-1 and HEV-3 mutants with introduced FHF-associated mutations (Fig. 8), suggesting that the FHF-associated mutations do not alter the RBV sensitivity, and therefore RBV treatment remains a viable option in FHF patients. However, considering the mutagenic effects of RBV, its administration in FHF patients should be very prudent (5, 6, 18, 19). Moreover, RBV use is precluded in pregnant women because of its teratogenic effects. Development of an effective HEV-specific antiviral for the treatment of FHF patients, especially in pregnant women, remains a top priority (52).

In conclusion, we determined the precise location and epidemiological prevalence of 11 FHF-associated mutations in distinct HEV genotypes. We systematically compared the replication ability, infectivity, and antiviral sensitivity of different HEV mutants with single or double FHF-associated mutations and demonstrated that only two of the 11 FHF-associated mutations, A317T and V1120I, enhanced HEV-1 replication efficiency. Importantly, both mutations simultaneously occurred in all 21 tightly clustered HEV-1 strains that are associated with FHF in patients from outbreaks in Bangladesh, suggesting that these two mutations may associate with FHF. Our data provide direct experimental evidence that two FHF-associated HEV-1 mutations may link to the rapid viral transmission and FHF in endemic regions.

Materials and Methods

Sequence Analyses. A total of 953 complete viral genomes of four HEV genotypes (82 genomes for HEV-1; 2 genomes for HEV-2; 644 genomes for HEV-3; and 225 genomes for HEV-4) analyzed in this study were downloaded in the GenBank database (retrieved as of June 2022). Genomic sequences from each genotype were aligned using the MAFFT algorithm in Geneious Prime software version 2022.1.1. Nucleotide and amino acid numberings are according to the genomic sequence of HEV reference strain Burma (GenBank no. M73218) (10). Locations of functional domains and motifs within HEV ORF1 are according to the Burma strain (26).

HEV Infectious Clones and Indicator Replicons. The HEV-1 infectious cDNA clone (designated Sar55) is derived from the Sar55 strain (GenBank accession no. AF444002) (31), and the HEV-3 infectious clone (designated p6) is derived from the Kernow-C1 strain (GenBank accession no. JQ679013), which has been consecutively passaged six times in cell culture (35). The HEV-1 Sar55 and HEV-3 p6 infectious clones, gifts from Sue Emerson, National Institute of Allergy and Infectious Diseases, NIH, have been extensively used in previous studies (17, 18, 20, 28, 31, 34, 35). The HEV-1 indicator replicon (designated Sar55Gluc) was generated based on the HEV-1 Sar55 infectious clone backbone whose partial ORF2 was replaced by the *Gaussia* luciferase gene, which is a gift from Alexander Ploss, Princeton University, Princeton, NJ) (29). Likewise, the HEV-3 indicator replicon (designated p6Gluc) is generated using the p6 infectious clone backbone, which has been described previously (31, 34).

Additional materials and methods are described in *SI Appendix*.

Data, Materials, and Software Availability. All study data are included in the article and/or supporting information.

ACKNOWLEDGMENTS. We thank Dr. Sue Emerson (NIAID, NIH) for kindly providing the HEV-1 Sar55 and HEV-3 p6 infectious clones, HEV-3 p6 *Gaussia* luciferase indicator replicon, and Huh7-S10-3 cells. We also thank Dr. Alexander

Ploss (Princeton University) for kindly providing the HEV-1 Sarr55 *Gaussia* luciferase indicator replicon. The authors' research on HEV is funded by a grant from the NIH (R01 AI050611).

Author affiliations: ^aDepartment of Biomedical Sciences and Pathobiology, Virginia-Maryland College of Veterinary Medicine, Virginia Polytechnic Institute and State University, Blacksburg, VA 24061; and ^bCenter for Emerging, Zoonotic and Arthropod-Borne Pathogens, Virginia Polytechnic Institute and State University, Blacksburg, VA 24061

1. I. Nimgaonkar, Q. Ding, R. E. Schwartz, A. Ploss, Hepatitis E virus: Advances and challenges. *Nat. Rev. Gastroenterol. Hepatol.* **15**, 96–110 (2018).
2. R. H. Westbrook, G. Dusheiko, C. Williamson, Pregnancy and liver disease. *J. Hepatol.* **64**, 933–945 (2016).
3. M. S. Khuroo, Hepatitis E and pregnancy: An unholy alliance unmasked from Kashmir, India. *Viruses* **13** (2021).
4. N. Kamar *et al.*, Hepatitis E virus and chronic hepatitis in organ-transplant recipients. *N. Engl. J. Med.* **358**, 811–817 (2008).
5. D. Todt, T. L. Meister, E. Steinmann, Hepatitis E virus treatment and ribavirin therapy: Viral mechanisms of nonresponse. *Curr. Opin. Virol.* **32**, 80–87 (2018).
6. D. Todt, S. Walter, R. J. Brown, E. Steinmann, Mutagenic effects of ribavirin on hepatitis E virus-viral extinction versus selection of fitness-enhancing mutations. *Viruses* **8**, 283 (2016).
7. S. Lhomme, F. Abravanel, P. Cintas, J. Izopet, Hepatitis E virus infection: Neurological manifestations and pathophysiology. *Pathogens* **10**, 1582 (2021).
8. M. A. Purdy *et al.*, ICTV virus taxonomy profile: *Hepeviridae* 2022. *J. Gen. Virol.*, in press.
9. B. Wang, X. J. Meng, Hepatitis E virus: Host tropism and zoonotic infection. *Curr. Opin. Microbiol.* **59**, 8–15 (2021).
10. D. B. Smith *et al.*, Update: Proposed reference sequences for subtypes of hepatitis E virus (species *Orthohepevirus A*). *J. Gen. Virol.* **101**, 692–698 (2020).
11. H. Sooryanarain, X. J. Meng, Hepatitis E virus: Reasons for emergence in humans. *Curr. Opin. Virol.* **34**, 10–17 (2019).
12. A. B. Brayne, B. L. Dearlove, J. S. Lester, S. L. Kosakovsky Pond, S. D. W. Frost, Genotype-specific evolution of hepatitis E virus. *J. Virol.* **91**, e02241-16 (2017).
13. B. Wang, X. J. Meng, Structural and molecular biology of hepatitis E virus. *Comput. Struct. Biotechnol. J.* **19**, 1907–1916 (2021).
14. V. P. Nair *et al.*, Endoplasmic reticulum stress induced synthesis of a novel viral factor mediates efficient replication of genotype-1 hepatitis E virus. *PLoS Pathog.* **12**, e1005521 (2016).
15. J. Scholz, A. Falkenhagen, C. T. Bock, R. Johnne, Reverse genetics approaches for hepatitis E virus and related viruses. *Curr. Opin. Virol.* **44**, 121–128 (2020).
16. T. L. Meister, J. Bruening, D. Todt, E. Steinmann, Cell culture systems for the study of hepatitis E virus. *Antiviral Res.* **163**, 34–49 (2019).
17. Y. Debing *et al.*, Hepatitis E virus mutations associated with ribavirin treatment failure result in altered viral fitness and ribavirin sensitivity. *J. Hepatol.* **65**, 499–508 (2016).
18. D. Todt *et al.*, In vivo evidence for ribavirin-induced mutagenesis of the hepatitis E virus genome. *Gut* **65**, 1733–1743 (2016).
19. S. Lhomme *et al.*, Mutation in the hepatitis E virus polymerase and outcome of ribavirin therapy. *Antimicrob. Agents Chemother.* **60**, 1608–1614 (2015).
20. Y. Debing *et al.*, A mutation in the hepatitis E virus RNA polymerase promotes its replication and associates with ribavirin treatment failure in organ transplant recipients. *Gastroenterology* **147**, 1008–11.e7, quiz e15–e16 (2014).
21. H. van Tong *et al.*, Hepatitis E virus mutations: Functional and clinical relevance. *EBioMedicine* **11**, 31–42 (2016).
22. N. Kamar *et al.*; Hepatitis E Virus Ribavirin Study Group, Ribavirin for hepatitis E virus infection after organ transplantation: A large European retrospective multicenter study. *Clin. Infect. Dis.* **71**, 1204–1211 (2020).
23. N. Mishra, A. M. Walimbe, V. A. Arankalle, Hepatitis E virus from India exhibits significant amino acid mutations in fulminant hepatic failure patients. *Virus Genes* **46**, 47–53 (2013).
24. J. Borkakoti, G. Ahmed, P. Kar, Report of a novel C1483W mutation in the hepatitis E virus polymerase in patients with acute liver failure. *Infect. Genet. Evol.* **44**, 51–54 (2016).
25. J. Borkakoti, G. Ahmed, A. Rai, P. Kar, Report of novel H105R, D29N, V27A mutations in the methyltransferase region of the HEV genome in patients with acute liver failure. *J. Clin. Virol.* **91**, 1–4 (2017).
26. E. V. Koonin *et al.*, Computer-assisted assignment of functional domains in the nonstructural polyprotein of hepatitis E virus: Delineation of an additional group of positive-strand RNA plant and animal viruses. *Proc. Natl. Acad. Sci. U.S.A.* **89**, 8259–8263 (1992).
27. B. Wang *et al.*, A new hepatitis E virus genotype 2 strain identified from an outbreak in Nigeria, 2017. *Virol. J.* **15**, 163 (2018).
28. D. Todt *et al.*, Robust hepatitis E virus infection and transcriptional response in human hepatocytes. *Proc. Natl. Acad. Sci. U.S.A.* **117**, 1731–1741 (2020).
29. Q. Ding *et al.*, Identification of the Intragenomic Promoter Controlling Hepatitis E Virus Subgenomic RNA Transcription. *MBio* **9**, e00769-18 (2018).
30. X. Ju *et al.*, Identification of functional cis-acting RNA elements in the hepatitis E virus genome required for viral replication. *PLoS Pathog.* **16**, e1008488 (2020).
31. H. T. Nguyen, P. Shukla, U. Torian, K. Faulk, S. U. Emerson, Hepatitis E virus genotype 1 infection of swine kidney cells in vitro is inhibited at multiple levels. *J. Virol.* **88**, 868–877 (2014).
32. B. Wang *et al.*, Comprehensive molecular approach for characterization of hepatitis E virus genotype 3 variants. *J. Clin. Microbiol.* **56**, e01686-17 (2018).
33. T. N. Hoa *et al.*, A tightly clustered hepatitis E virus genotype 1a is associated with endemic and outbreak infections in Bangladesh. *PLoS One* **16**, e0255054 (2021).
34. P. Shukla *et al.*, Cross-species infections of cultured cells by hepatitis E virus and discovery of an infectious virus-host recombinant. *Proc. Natl. Acad. Sci. U.S.A.* **108**, 2438–2443 (2011).
35. P. Shukla *et al.*, Adaptation of a genotype 3 hepatitis E virus to efficient growth in cell culture depends on an inserted human gene segment acquired by recombination. *J. Virol.* **86**, 5697–5707 (2012).
36. X. Yin, C. Ambardekar, Y. Lu, Z. Feng, Distinct entry mechanisms for nonenveloped and quasi-enveloped hepatitis E viruses. *J. Virol.* **90**, 4232–4242 (2016).
37. S. Lhomme *et al.*, Characterization of the polyprotein region of the hepatitis E virus in immunocompromised patients. *J. Virol.* **88**, 12017–12025 (2014).
38. M. K. Parvez, Mutational analysis of hepatitis E virus ORF1 “Y-domain”: Effects on RNA replication and virion infectivity. *World J. Gastroenterol.* **23**, 590–602 (2017).
39. M. S. Khuroo, M. R. Teli, S. Skidmore, M. A. Sofi, M. I. Khuroo, Incidence and severity of viral hepatitis in pregnancy. *Am. J. Med.* **70**, 252–255 (1981).
40. S. P. Jaiswal, A. K. Jain, G. Naik, N. Soni, D. S. Chitnis, Viral hepatitis during pregnancy. *Int. J. Gynaecol. Obstet.* **72**, 103–108 (2001).
41. A. B. Aziz, S. Hamid, S. Iqbal, W. Islam, S. A. Karim, Prevalence and severity of viral hepatitis in Pakistani pregnant women: A five year hospital based study. *J. Pak. Med. Assoc.* **47**, 198–201 (1997).
42. M. H. Wißing, Y. Brüggemann, E. Steinmann, D. Todt, Virus-host cell interplay during hepatitis E virus infection. *Trends Microbiol.* **29**, 309–319 (2021).
43. S. Lhomme *et al.*, Hepatitis E pathogenesis. *Viruses* **8**, 212 (2016).
44. N. Jilani *et al.*, Hepatitis E virus infection and fulminant hepatic failure during pregnancy. *J. Gastroenterol. Hepatol.* **22**, 676–682 (2007).
45. H. Sooryanarain, S. A. Ahmed, X. J. Meng, Progesterone-mediated enhancement of hepatitis E virus replication in human liver cells. *MBio* **12**, e0143421 (2021).
46. S. B. Prabhu *et al.*, Study of cellular immune response against Hepatitis E virus (HEV). *J. Viral Hepat.* **18**, 587–594 (2011).
47. P. Devhare, K. Sharma, V. Mhaidarkar, V. Arankalle, K. Lole, Analysis of helicase domain mutations in the hepatitis E virus derived from patients with fulminant hepatic failure: Effects on enzymatic activities and virus replication. *Virus Res.* **184**, 103–110 (2014).
48. B. A. Tannous, *Gaussia* luciferase reporter assay for monitoring biological processes in culture and in vivo. *Nat. Protoc.* **4**, 582–591 (2009).
49. N. Shao, R. Bock, A codon-optimized luciferase from *Gaussia princeps* facilitates the in vivo monitoring of gene expression in the model alga *Chlamydomonas reinhardtii*. *Curr. Genet.* **53**, 381–388 (2008).
50. S. Lhomme *et al.*, Hepatitis E Virus: How It Escapes Host Innate Immunity. *Vaccines (Basel)* **8**, 422 (2020).
51. D. B. Smith, P. Simmonds, Hepatitis E virus and fulminant hepatitis—a virus or host-specific pathology? *Liver Int.* **35**, 1334–1340 (2015).
52. V. Kinast, T. L. Burkard, D. Todt, E. Steinmann, Hepatitis E virus drug development. *Viruses* **11**, 485 (2019).